



**scirocco**  
scatterometer instrument  
competence centre

# Scatterometer Instrument Competence Centre (SCIROCCO)

Research Grant Call 2015  
Final Report

## Research activity

Comparison of satellite soil moisture products, models and on-site observation by triple / quadruple collocation including ERS-ESCAT data over H-SAF region (Europe) and "globally" (for ESCAT regional scenario)

## Researcher

Fabio Fascetti

## Advisor

Ing. Raffaele Crapolicchio (Serco S.p.A.), MSc. Christoph Reimer (TUWien), Prof. Nazzareno Pierdicca (Sapienza)

## Date

28 October, 2016

## Document number

SCI-REP-16-0002

The work has been funded by an educational grant in the frame of the ESA Contract "Setup of the Scatterometer Instrument Competence Centre - SCIROCCO".

## Executive Summary

The first part of this research activity was carried out at the Technical University of Wien (TU Wien, Research Group Remote Sensing, Department for Geodesy and Geoinformation) for a period of three months, starting by March 2016, and it was continued at Sapienza University of Rome, until August 2016. The managing institution was Serco S.p.A. and Sapienza University. The aim of this work was to assess the quality of soil moisture products provided by active and passive satellite sensors, as ERS-2 ESCAT and SMOS data, in order to consolidate current methodologies for scatterometer data processing and calibration. For such purpose, several techniques, as Triple (TC) and Quadruple (QC) collocation, were used.

In particular, the ERS-2 ESCAT derived soil moisture products were compared with those provided by other microwave satellite sensors, as SMOS and AMSR-E, and by land surface model, as ERA Interim/Land produced by ECMWF. For the ERS-2 ESCAT soil moisture products both high and nominal resolutions were considered. Depending on the availability of the sensors, the Triple and Quadruple Collocation technique were used in order to estimate the error standard deviations of each system. In particular, when four systems were considered, the Extended Collocation (EC) was also used in order to take into account a possible error correlation factor between the soil moisture retrievals of the two radiometers of SMOS and AMSR-E. The analysis was accomplished considering a global scenario for a period starting from January 2010 to July 2011; the overlapping between the considered sensors, in particular for the satellite products, has constrained the time and spatial coverage of analysis. The TC, QC and EC results showed consistent error patterns in accordance with the error trend found in several literature works. In general, SMOS presented robust retrievals over dry areas and over specific land cover (as shrubland and grassland), while the scatterometer and the model presented better performance over moderately vegetated areas.

## **Abstract:**

In this work, the ERS-2 ESCAT derived soil moisture products were compared with those provided by other microwave satellite sensors, as SMOS and AMSR-E, and by land surface model, as ERA Interim/Land produced by ECMWF. For the ERS-2 ESCAT soil moisture products were considered both high (25 Km) and nominal resolutions (50 Km). The overlapping between the considered sensors, in particular for the satellite products, has constrained the time and spatial coverage of analysis, which was accomplished considering a global scenario for a period starting from January 2010 to July 2011. Depending on the availability of the sensors, the Triple (TC) and Quadruple (QC) Collocation technique were used in order to estimate the error standard deviations of each system. In particular, when four systems were considered, the Extended Collocation (EC) was also used in order to take into account a possible error correlation factor between the soil moisture retrievals of the two radiometers of SMOS and AMSR-E. The TC, QC and EC results showed consistent error patterns in accord with the error trend found in several literature works. In general, SMOS presented robust retrievals over dry areas and over specific land cover (as shrubland and grassland), while the scatterometer and the model presented better performance over the most of Europe and Norther-Est of America.

## **Datasets and pre-processing steps:**

### *SMOS*

The payload on-board the Soil Moisture Ocean Salinity (SMOS) satellite is the Microwave Imaging Radiometer using Aperture Synthesis (MIRAS) instrument; it is an interferometric radiometer that measures the cross-correlation between pairs of receivers to derive a visibility function (Kerr et al., 2001; Kerr et al., 2012). Such system operates at L-band (1.427 GHz) from an orbit of 758 km, with a horizontal spatial resolution between 35 and 50 km and a repetition time of 3 days. The satellite orbit is polar, crossing the equator at 06:00 am Local Solar Time (LST) for the

ascending passage and at 06:00 pm LST for the descending passage. The reprocessed ESA L2 product, which provides an actual volumetric moisture content (SMC, in  $\text{m}^3/\text{m}^3$ ), are sampled over the ISEA4h9 grid, which has a spacing in the order of 15 km (Kidd, 2005). The soil moisture products considered in this work were generated by the processor version 6.20, which introduced several improvements respect to the previous 5.51 version; in particular, more details can be found at the [https://earth.esa.int/documents/10174/1854503/SMOS\\_L2SMv620\\_release\\_note](https://earth.esa.int/documents/10174/1854503/SMOS_L2SMv620_release_note) website.

#### *AMSR-E*

The Advanced Microwave Scanning Radiometer – Earth Observing System (AMSR-E) is a radiometer on board of the NASA's Aqua satellite and stopped producing data in October 2011. The data were acquired at a single incidence angle ( $55^\circ$ ) operating at six wavelengths (89, 36.5, 23.8, 18.7, 10.65 and 6.925 GHz) in both horizontal and vertical polarizations; in this work, the retrievals at C-Band were used. The total swath is around 1445 km for each overpass, with a footprint resolutions ranging from 5 km (89 GHz) to 56 km (6.925 GHz). The satellite orbit is sun-synchronous with a morning (descending orbit) and afternoon (ascending orbit) overpasses at around 01:30 am/pm. In this study, the AMSR-E soil moisture retrievals derived according to the Land Parameter Retrieval Model (LPRM, Owe et al., 2001) version 5 were used.

#### *ERS2 – ESCAT*

The Active Microwave Instrument (AMI) on-board the European Remote Sensing satellites (ERS-1/2) included a wind scatterometer (ESCAT), which provided radar backscattering coefficients at C-Band (5.6 GHz). Three scatterometer antennas were pointed at  $45^\circ$  (fore),  $90^\circ$  (mid) and  $135^\circ$  (aft) with respect to the satellite flight direction, illuminating continuously a 500 km wide swath. The ERS satellite was characterized by a morning (descending orbit) and evening (ascending orbit) at 10:30 am/pm, with a varying repeat coverage of about 2 to 8 days. The ESCAT Level-2 surface soil moisture data were generated using the Water Retrieval Package (WARP) version 5.6, developed at the Technical University of Wien (TUWien, Research Group

Remote Sensing, Department for Geodesy and Geoinformation). The soil moisture retrievals are based on a change detection approach (Wagner et al., 1999) and they are derived in a relative value between 0 and 100%, which represent the driest and wettest soil conditions registered for each pixel. Then, the unit of ESCAT soil moisture products is a degree of saturation (%), which can be converted (when needed) into volumetric units ( $m^3m^{-3}$ ) through the soil porosity information. In this work, both the data at nominal resolution (50 km) and at high resolution (25 km) were used.

### *Soil Porosity*

The soil porosity information was obtained from the map available from the Global Land Data Assimilation System (GLDAS) website (<http://ldas.gsfc.nasa.gov/gldas/>), based on the Food and Agriculture (FAO) Soil Map of the World. The map is provided at 1/4 and 1° horizontal resolution and it was resampled over the WARP grid in order to associate its value to each ERS-2 ESCAT point.

### *ERA-Interim/Land*

The ERA-Interim/land is produced by the European Centre for Medium-Range Weather Forecasts (ECMWF) and it represents a global atmospheric reanalysis combined with an ocean and a land surface model (LSM). In particular, such product is produced starting from the ERA-Interim reanalysis and incorporating recent land model developments at the ECMWF combined with precipitation bias correction based on the Global Precipitation Climatology Project version 2.2 (GPCP v.2.2). Soil moisture is provided at four different layers and four time steps (at 00:00, 06:00, 12:00 and 18:00 UTC) each day over a grid with a space sampling of  $0.75 \times 0.75^\circ$  (Balsamo et al., 2015). In this work, the data interpolated over a fixed grid with a resolution of  $0.125 \times 0.125^\circ$  were used.

### *Data Collocation and pre-processing*

As a first step, the datasets were collocated in space and in time, choosing SMOS as reference. Then, the ERS-2 ESCAT, AMSR-E and ERA-Interim/Land products were resampled over the ISEA4h9 grid, characterized by a space sampling around 15 km; for such purpose, a nearest neighbour approach was used. Moreover, only data fulfilling the following conditions were retained into the analysis: *i*) SMOS, AMSR-E and ERA-Interim/Land retrievals between 0 and 0.7 m<sup>3</sup>/m<sup>3</sup> (as greater values are not plausible); *ii*) SMOS retrievals with Data Quality Index (DQX) less than 0.045; *iii*) ERS-2 ESCAT retrievals not frozen and without backscattering corrections considering the provided quality flags of the soil processor. The latter point was accomplished using the information of the Surface State Flag (SSF), correction and processing flag provided by ERS-2 product.

The soil moisture anomalies ( $\vartheta_{anomaly}$ ) were evaluated through a moving window with a temporal size of N equal to 35 days ( $\vartheta_N^{doi}$ ), i.e. 17 before and 17 after respect the considered day of interest (doi), as indicated in equation (1).

$$\vartheta_{anomaly} = \vartheta_{doi} - \vartheta_N^{doi} \quad (1)$$

Such window width is able to capture the cycle of the soil moisture and then to isolate its anomaly; in literature, a large number of works used a similar value as width for the temporal window (for instance, in Dorigo et al., 2010 and Miralles et al., 2010).

An overall picture of the quantity of collocated data is shown in Fig.1, where in each ISEA4h9 grid point the number of triple (SMOS, ERS-2 and ERA-Interim/Land) and quadruple collocations (SMOS, ERS-2, ERA-Interim/Land and AMSR-E) are represented. It is worth to underline that the number of collocations were basically determined by the satellites and constrained mainly by their orbit overlapping. In particular, in the case of the QC scenario (lower panel of Fig.1), it is possible to note an evident decrease in the numbers of collocations for each grid point and such effect can be addressed to the observation period, which was restricted only to morning passages. Indeed, the afternoon descending passages of AMSR-E are around



the 01:30 PM LST, characterized by thermal conditions very different from that of the others satellite passages (10:30 pm for ERS-2 and 06:00 pm for SMOS). Then, in order to analyse soil moisture retrievals provided in similar conditions, a good strategy is to use only the morning passages for each satellite (01:30 am for AMSR-E, 06:00 am for SMOS and 10:30 am for ERS-2); a similar choice was also made in Dorigo et al., 2010.

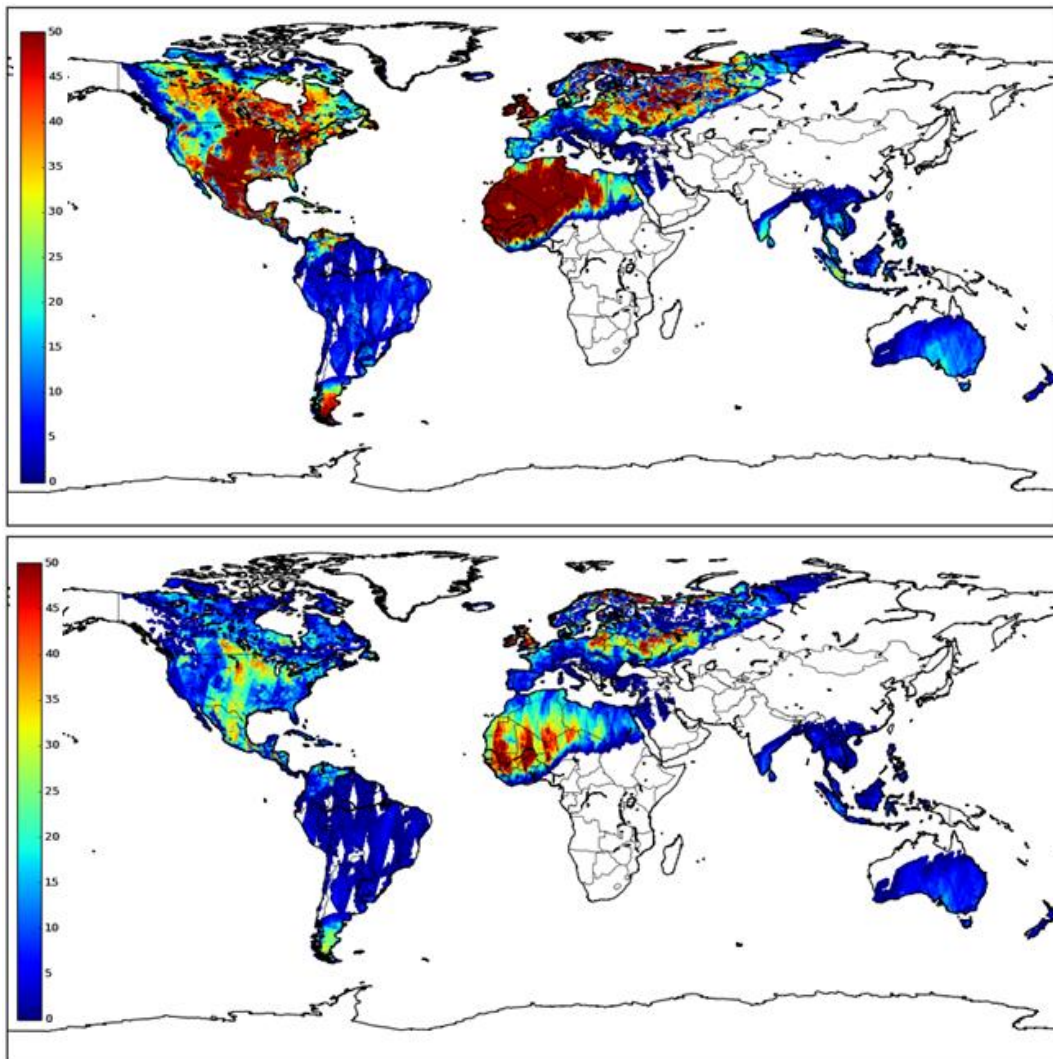


Fig.1: Number of collocations, indicated by the colorbar, of SMOS, ERS-2 and ERA-Interim/Land (upper panel) and of SMOS, ERS-2, ERA-Interim/Land and AMSR-E (lower panel) estimated in each point of the ISEA4h9 grid in the considered time frame (January 2010 – July 2011).

In some regions, like Australia, South America or Central Europe, the number of collocations is very poor, mainly due to the ERS-ESCAT mission operated in regional mission scenario and probably not sufficient to provide an accurate sampling of soil moisture for its error characterization. However, the TC and QC techniques were also applied over these kind of areas, taking into account the low number of collocations for the interpretation of the error trend, which were also compared with literature results in order to analyse their consistency.

### **Triple Collocation Results**

The pointwise TC was applied to the SMOS, ERS-2 (high resolution) products and the LSM outputs, independently for each grid point of the collocated maps. In this way, the capability to reproduce the soil moisture temporal variability is evaluated, assuming that in each point the gain and bias parameters of each measurement system can be separate with respect to the chosen reference system. This is a usual practice found in the literature dealing with soil moisture or rain rate retrievals (i.e., Dorigo et al., 2010).

The error standard deviations estimated by the TC can be simply related to the combination of the correlation coefficients between the systems (as highlighted in Pierdicca et al., 2015a) and then, such maps as reported in Fig.2 can be produced in order to have a preliminary overview of the systems behaviour.



Comparison of satellite soil moisture products, models and on-site observation by triple / quadruple collocation including ERS-ESCAT data over H-SAF region (Europe) and "globally" (for ESCAT regional scenario)

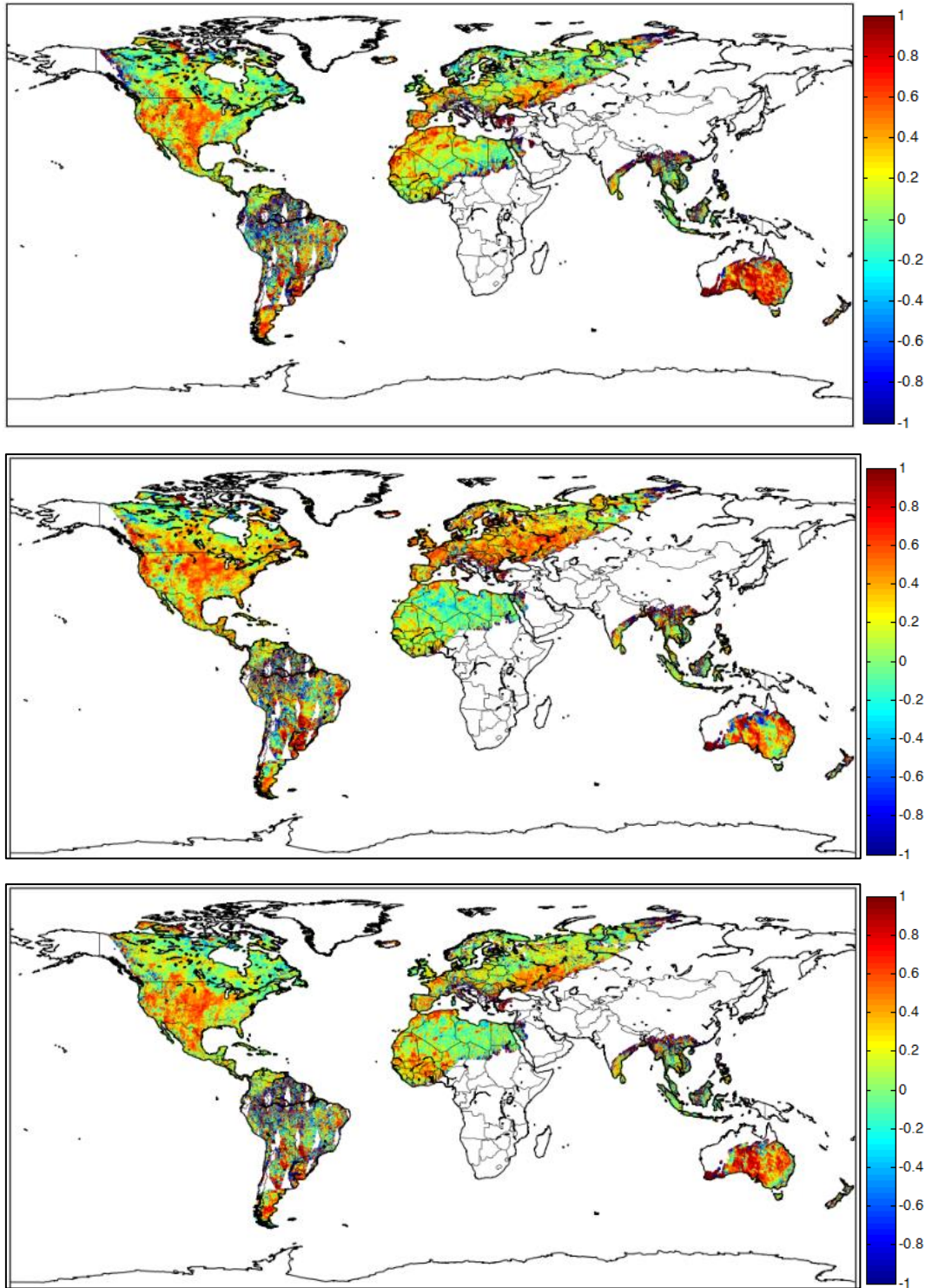


Fig.2: Maps of the pointwise correlation coefficient between SMOS and ERA-Interim/Land (first row), ERS-2 and ERA-Interim/Land (middle row) and SMOS and ERS-2 (lower row).

Comparison of satellite soil moisture products, models and on-site observation by triple / quadruple collocation including ERS-ESCAT data over H-SAF region (Europe) and "globally" (for ESCAT regional scenario)

Comparing these correlation maps with the land cover information provided by the European Space Agency Climate Change Initiative project (i.e., ESA CCI land cover map, available at <http://maps.elie.ucl.ac.be/CCI/viewer/> website), a dependence of the correlation behaviour with respect to the soil cover can be observed. Indeed, observing Fig.3, which represents a zoom of the Fig.2 over the Northern America, the pattern of the land cover can be simply recognized from the correlation map. In particular, it can be noted that soil moisture retrievals show more agreement over not densely vegetated areas.

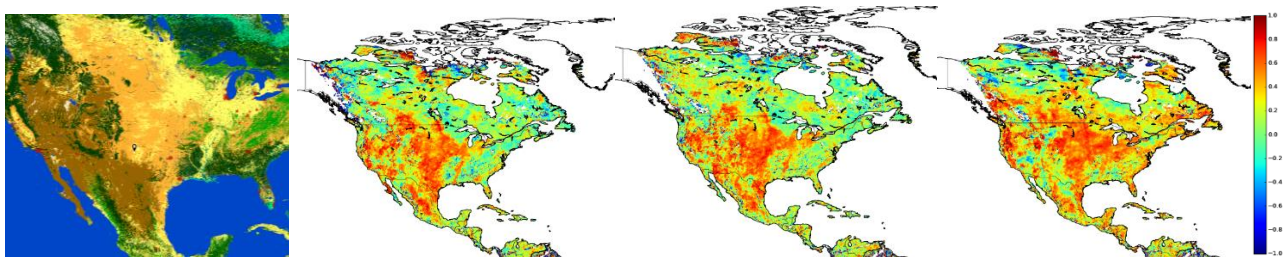


Fig.3 : In order from the left: CCI Land Cover map (shrubland in brown, cropland in yellow, grassland in orange and tree covered in green); Correlation maps between SMOS and ERA-Interim/Land, SMOS and ERS-2, ERS-2 and ERA-Interim/Land.

Fig.4 reports the error standard deviation of each system evaluated through the TC. For this analysis, SMOS was chosen as reference and then the errors are represented in the scale of SMOS. The maps report the pointwise error standard deviations for each system, analysing only points in which the results make sense, i.e. with a positive estimation of the error variances. In general, SMOS presented the best performance in most of dry regions respect to the other systems, as in Northern Africa and in Australia, whereas the model and the scatterometer showed low patterns of error in the East of Northern America and in the most parts of Europe.

Comparison of satellite soil moisture products, models and on-site observation by triple / quadruple collocation including ERS-ESCAT data over H-SAF region (Europe) and "globally" (for ESCAT regional scenario)

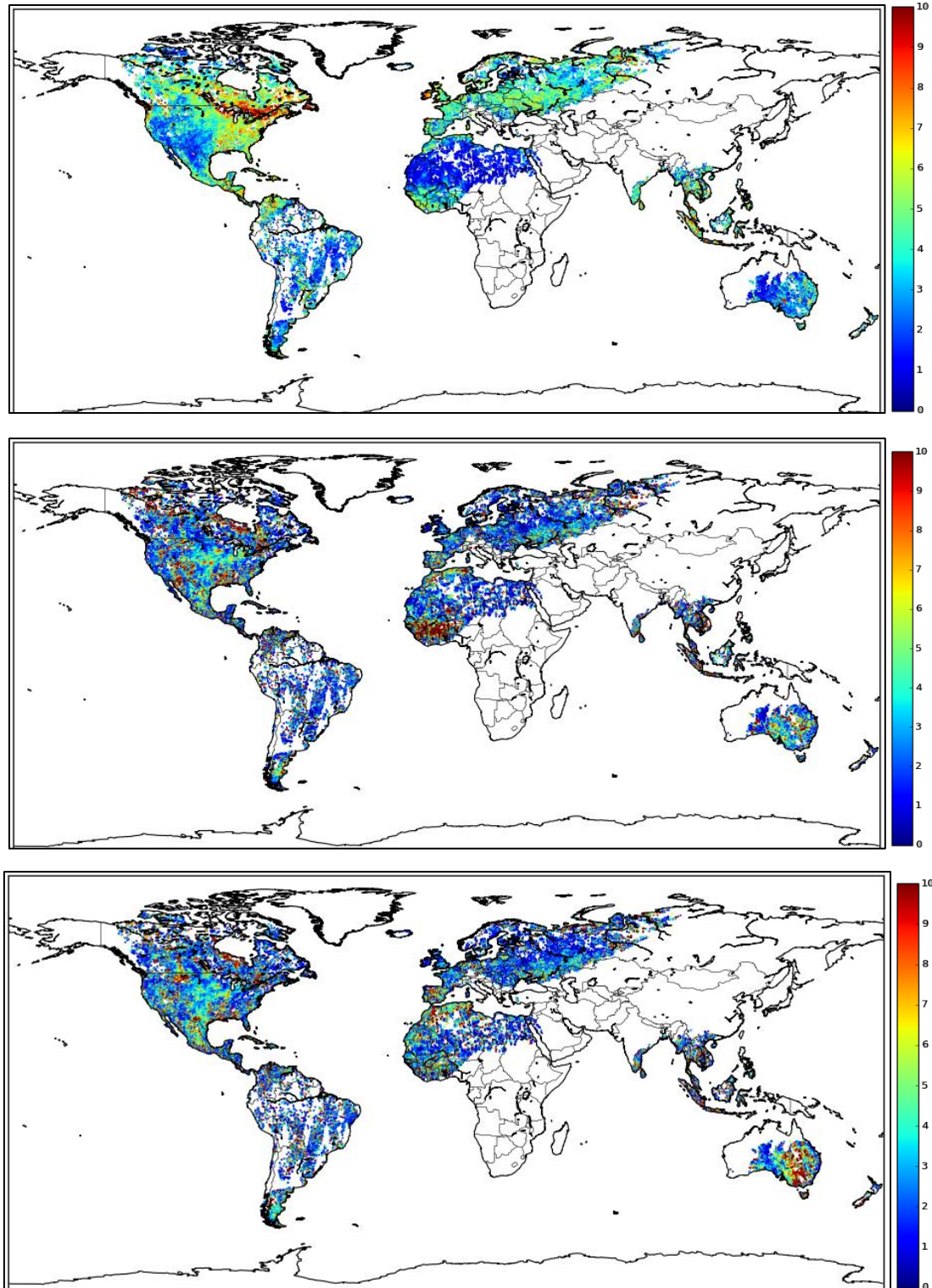


Fig.4 : Error standard deviations in % of SMOS (upper row on the left), ERA-Interim/Land (upper row on the right) and ERS-2 (lower panel). SMOS is the reference of the TC analysis.



Focusing on Northern America, the SMOS error standard deviation presented an evident trend change, like a vertical cut, and this effect is in correspondence of the change of the land cover class. Such results showed a more robust SMOS estimation over shrubland and grassland with respect to tree covered regions ; Table 1 reports the mean of the error standard deviations for each systems, considering several land cover classes for the global scenario.

Table 1: mean of the error standard deviations evaluated through the TC approach depending on the considered land cover class over the whole global scenario.

Land cover class	SMOS [%]	ERA/Interim-Land [%]	ERS-2 [%]
Bare Soils	1.52	3.24	4.03
Grassland	3.67	4.08	3.82
Shrubland	2.65	5.73	4.27
Tree needleaved	5.00	5.49	4.08

Considering the European region, the patterns of the error standard deviations of the three systems showed coherent behaviour with respect to those evaluated in a previous work (Pierdicca et al.,2015a), where SMOS (v.5.51) and ERA-Interim/Land were compared with the Advanced SCATterometer (ASCAT) soil moisture products. In that case, SMOS showed good performance in the arid areas, like the Sahara desert and in the middle of the Spain. Instead, as underlined in Fig.4, the model and the scatterometer presented low error standard deviations over most parts of Europe. In Pierdicca et al., 2015a, a period of three years from 2010 to 2012 was analysed and a greater number of collocations for each grid point was found with respect to the present study. Comparing the results of these two works, the agreement of the error trends are consistent with the results presented in this report, even if the number of collocation is less than 50 for some grid point, as showed in Fig.1.

Morevoer, considering only SMOS and ERS-2 error standard deviations, areas in which either SMOS or ERS-2 present a lower error are represented in Fig.5 (right panel). It is interesting to note that such trends are consistent with respect to that

found in Al-Yaari et al., 2014 (left panel of Fig.5), where SMOS soil moisture retrievals were compared with the ASCAT products and simulations provided by the Modern ERA Retrospective analysis for Research and Applications (MERRA) Land model considering a period from 2010 to 2012. In general the trends are very similar, showing in both cases high performances for SMOS over sparse vegetation cover and lowest errors for the scatterometer over dense vegetation covers.

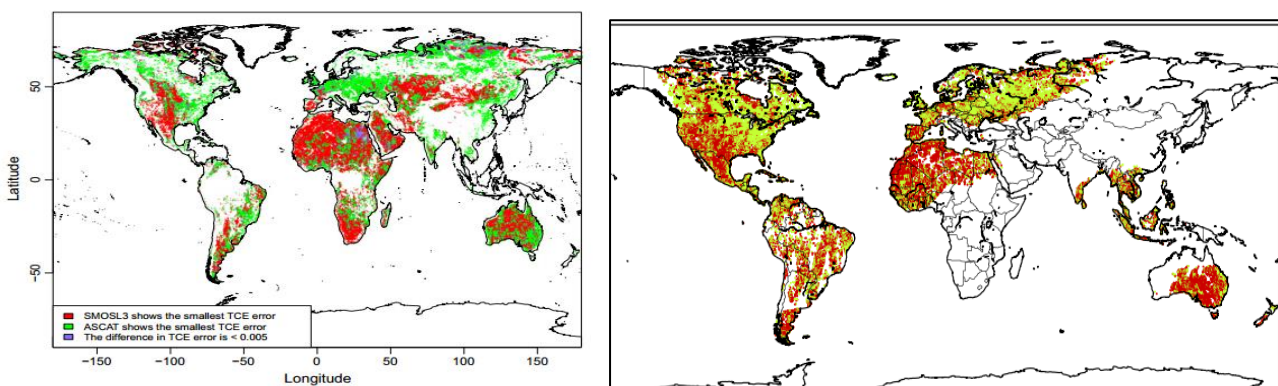


Fig.5 : Areas where: SMOS (red) or ASCAT (green) presents the lower error standard deviations (left panel), analysed in Al-Yaari, et al.,2014; SMOS (red) or ERS-2 (green) presents the lower error standard deviations (right panel).

Moreover, Table 2 reports the mean of the error standard deviations for each systems depending on the considered area in the world. In particular, Table 2 can be useful to analyse the error trend of each system by considering several areas characterized by different climatologic events, land cover and properties, as RFI presence. For example, SMOS resulted more performant over Australia respect to the other areas, and it could be due to the low RFI presence over such area.

Table 2: mean of the TC error standard deviations depending on the considered area of the world.

World Area	SMOS [%]	ERA/Interim-Land [%]	ERS-2 [%]
Europe and Northern Africa	4.22	3.98	3.92
Northern America	4.21	4.18	4.12

Australia 2.98 3.76 4.46

The pointwise TC analysis was also accomplished considering the ERS-2 at nominal resolution (i.e., around 50 km), resampled on the WARP grid. The trend of the correlation and error standard deviation maps showed similar patterns such as those previously reported, i.e. considering the ERS-2 products at high resolution; such maps are not here reported in order to avoid redundancy on the figures. However, it may be useful to observe the histogram of the pointwise differences between the error standard deviations values for each system, depending on the resolution of considered ERS-2 data; such histograms are reported in Fig.6. The differences were evaluated from the TC results obtained considering ERS-2 at high resolution minus those considering ERS-2 at nominal resolution.

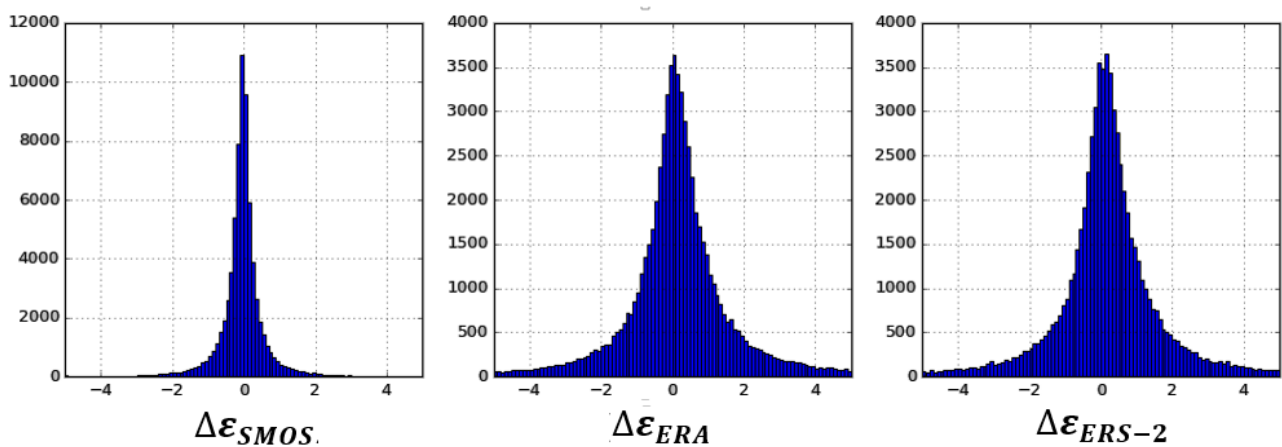


Fig.6: Histogram of the error standard deviation differences for SMOS ( $\Delta\epsilon_{SMOS}$ , on the left side), ERA/Interim-Land ( $\Delta\epsilon_{ERA}$ , on the middle) and ERS-2 ( $\Delta\epsilon_{ERS-2}$ , on the right side) products; the differences were evaluated considering the TC results using ERS-2 at high resolution minus the TC results using the nominal ERS-2 products.

The mean values of the distributions reported in Fig.6 are -0.05, 0.13 and 0.17 for SMOS, ERA/Interim-Land and ERS-2 products, respectively. From this analysis, the positive mean values of the ERS-2 histogram (greater with respect to the other two systems) is representative of a general better performance of the scatterometer when the low resolution data are considered. However, such results do not state that the

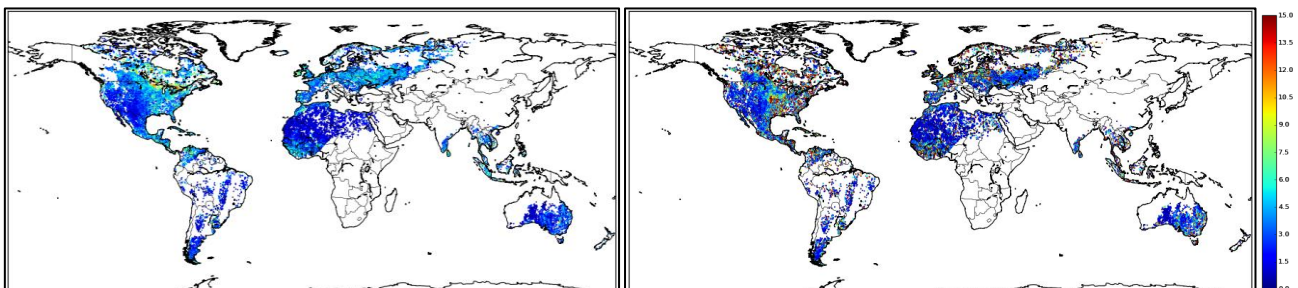


nominal ERS-2 data are more consistent with respect to those produced at high resolution, but such outcome can be addressed to the resolution of the other systems, which were considered into the TC analysis. Indeed, the nominal ERS-2 products present a resolution more similar to that of the other analysed datasets; then, the ERS-2 products at high resolution can be considered by the TC approach more noisily than the other systems.

### Quadruple Collocation results

The error standard deviations of the systems were also evaluated through a quadruple collocation analysis using the AMSR-E retrievals as fourth datasets. As mentioned before, in this case the analysis were limited only to morning passages, due to the equator crossing time of AMSR-E descending orbit; such choice was made in order to consider only the satellite soil moisture products retrieved in similar enviromental condition, even if the number of collocations strongly decreased. At the beginning, the QC technique was applied considering the error approach reported in Pierdicca et al., 2015b. Such technique allows to estimate the error standard deviations of four systems in an unique scale through the covariance and variance combinations of all the systems; for such purpose, the ERS-2 product was converted into volumetric soil moisture using the porosity information. Subsequently, the EC approach (Gruber et al., 2015) was applied to the same datasets in order to take into account the possibility of an error cross correlation between the two radiometers.

Fig.7 reports the error standard deviations in % for each systems evaluated through the QC. The error are expressed in the scale of SMOS, chosen as reference.



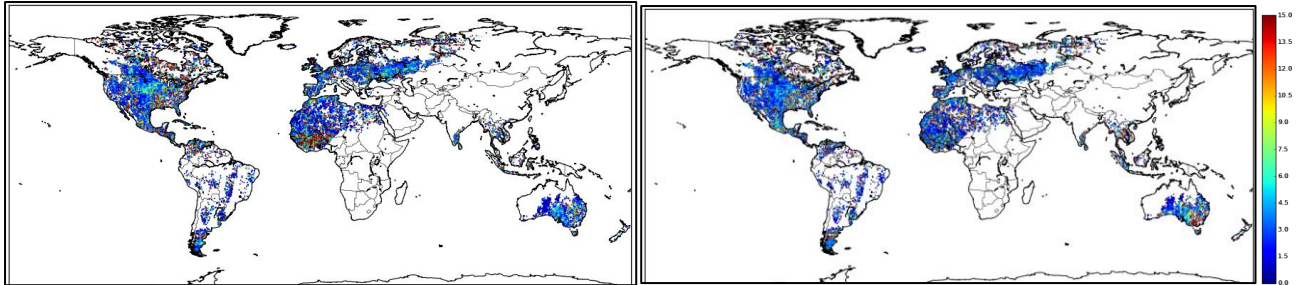


Fig.7: Error standard deviations in % of SMOS (right side of first row), AMSR-E (left side of first row), ERA-Interim/Land (right side of second row) and ERS-2 (left side of second row).

As expected, it is possible to recognize a similar error pattern comparing the TC and QC error standard deviation maps of SMOS, ERS-2 and ERA/Interim-Land; then, similar conclusions can be drawn for these datasets. In general, AMSR-E products showed low performance in the eastern parts of United States; such trend was also found in Gruber et al., 2016, where the ASCAT and Global Land Data Assimilation System (GLDAS) data were compared to AMSR-E products through a TC analysis.

Focusing on the analysis between ERS-2 and AMSR-E products, the right panel of Fig.8 represents the areas in which one of the two systems presented the lowest error (red for AMSR-E and blue for ERS). A same error representation was made in Dorigo et al., 2010, where the AMSR-E error standard deviation was estimated through a TC approach considering ERA/Interim model and ASCAT scatterometer data; the comparison between AMSR-E and ASCAT error standard deviations is reported on the left side of Fig.8. In general, the trends of the spatial error are very similar.

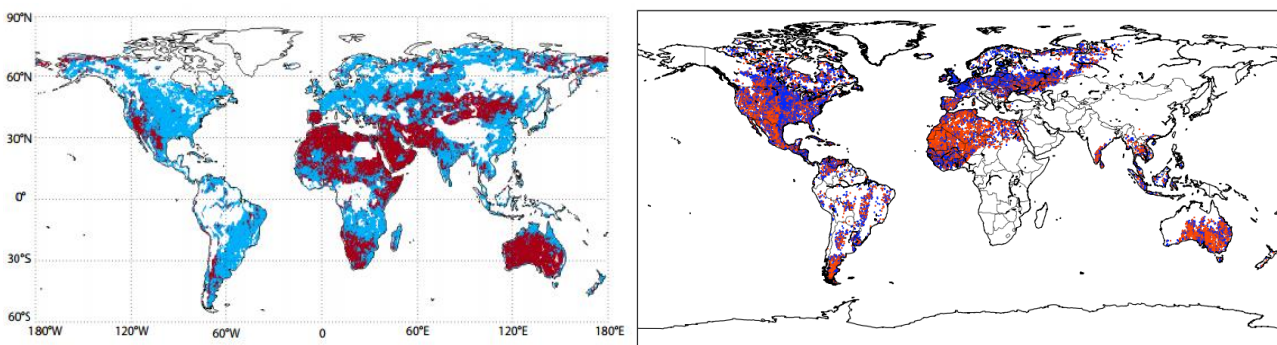


Fig.8: Areas where ASCAT (blue) or AMSR-E (red) presented the lower error standard deviations. The left panel represents the results evaluated in Dorigo et al., 2010, while the right panel shows the trend of the error estimated by the QC considering ERS-2 ESCAT (blue) and AMSR-E (red) data.

Table 3 reports the mean of the error standard deviations of the four systems evaluated through the QC analysis considering several global areas (the same of Table 2).

Table 3: mean of the QC error standard deviations of SMOS, AMSR-E, ERA/Interim-Land and ERS-2 ESCAT data depending on the considered area of the world. The errors are in the scale of SMOS.

World Area	SMOS [%]	AMSR-E [%]	ERA/Interim-Land [%]	ERS-2 [%]
Europe and Northern Africa	3.66	4.37	4.35	4.02
Northern America	3.53	4.47	4.50	4.18
Australia	2.47	3.41	3.51	4.26

It is worth to mention that the improvement of the SMOS error standard deviations with respect to the TC estimations reported in Table 2 could be related to the presence of a cross-correlation error with respect to the AMSR-E products. Such aspect will be discussed and analysed in the next section.

As for the TC analysis, the QC approach was carried out also considering the ERS-2 data at nominal resolution; the maps of error standard deviations are not reported in here to avoid redondance in the figures. Indeed, the behaviour of the error standard deviations (estimated through the QC) is very similar if either ERS-2 at nominal or high resolution were used.

However, the trend of the differences (depending on the resolution of the ERS-2 data) between the error standard deviations of each system were analysed and reported in Fig.9 in an histogram form, as made in Fig.6. The mean values of the distributions reported in Fig.9 are -0.03, 0.03, 0.06 and 0.16 for SMOS, AMSR-E,

ERA/Interim-Land and ERS-2 data, respectively; such trends highlight the conclusions derived by the TC approach.

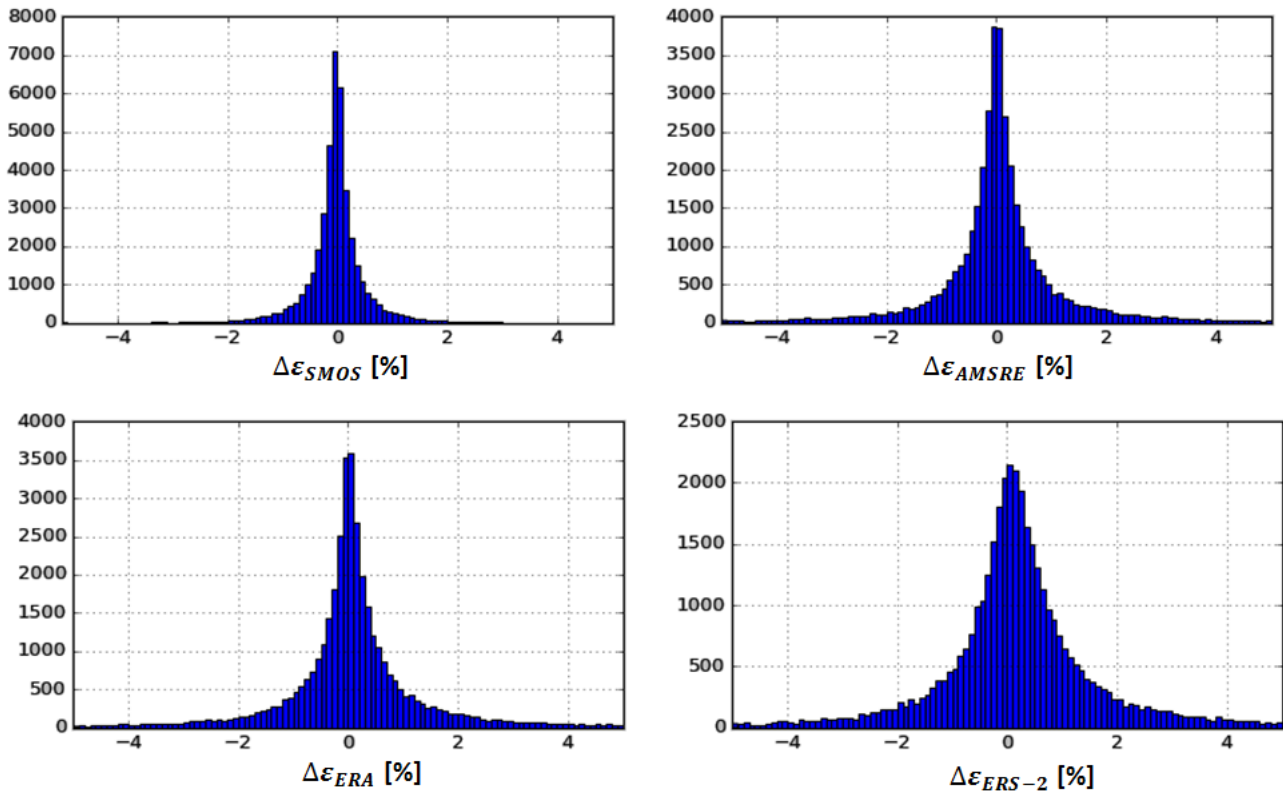


Fig.9: Histogram of the error standard deviation differences for SMOS ( $\Delta\epsilon_{SMOS}$ , on the left side of upper row), AMSR-E ( $\Delta\epsilon_{AMSR-E}$ , on the right side of upper row), ERA/Interim-Land ( $\Delta\epsilon_{ERA}$ , on left side of lower row) and ERS-2 ( $\Delta\epsilon_{ERS-2}$ , on the right side of lower row) products; the differences were evaluated considering the QC results using ERS-2 at high resolution minus the QC results using the nominal ERS-2 products.

Indeed, it can be noted that the difference between the ERS-2 error standard deviation (high resolution minus nominal resolution) present a positive mean value very different and greater with respect to the others. Such results can be due to the resolution of the new added system in order to apply the QC analysis: AMSR-E is characterized by a resolution more similar to that of the nominal ERS-2 products.



### Extended Collocation results

The extended collocation allows an estimation of the error standard deviations of more than three datasets through an average of all the possible TC combinations, which contain the analysed system. If two systems are supposed to present a cross-correlation error, the TC combination (containing such couple of systems) are not considered into the mean of the error evaluation, but its information is used to evaluate the error cross-covariance between these systems.

Then, as mentioned in the introduction, the SMOS and AMSR-E soil moisture retrievals are derived at two different frequencies (L- and C-band, respectively), but both the estimates start from radiometer measurements. Then, the hypothesis of not correlated errors between all the couples of systems could be not respected. For such purpose, the error standard deviations of the systems were also evaluated through the EC approach, considering a cross-correlation error between the SMOS and AMSR-E products.

Fig.10 shows the cross-correlation error between the two radiometers, estimated through the EC technique.

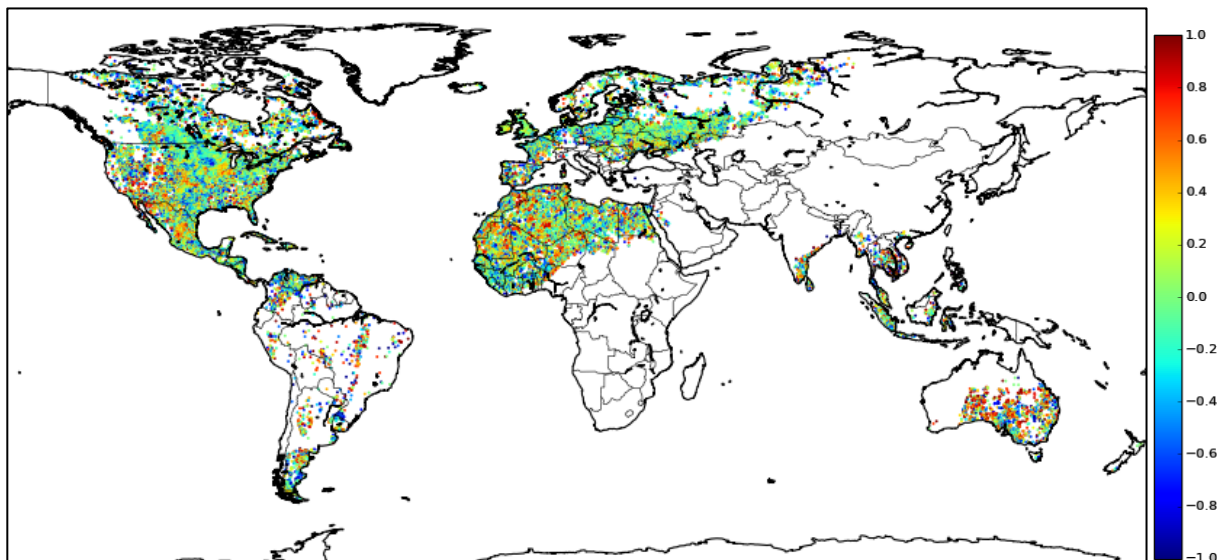


Fig.10: Error cross-correlation between SMOS and AMSR-E products estimated through the Extended Triple collocation.

The estimated error standard deviations of the four systems are reported in Fig.11; the errors are expressed in %.

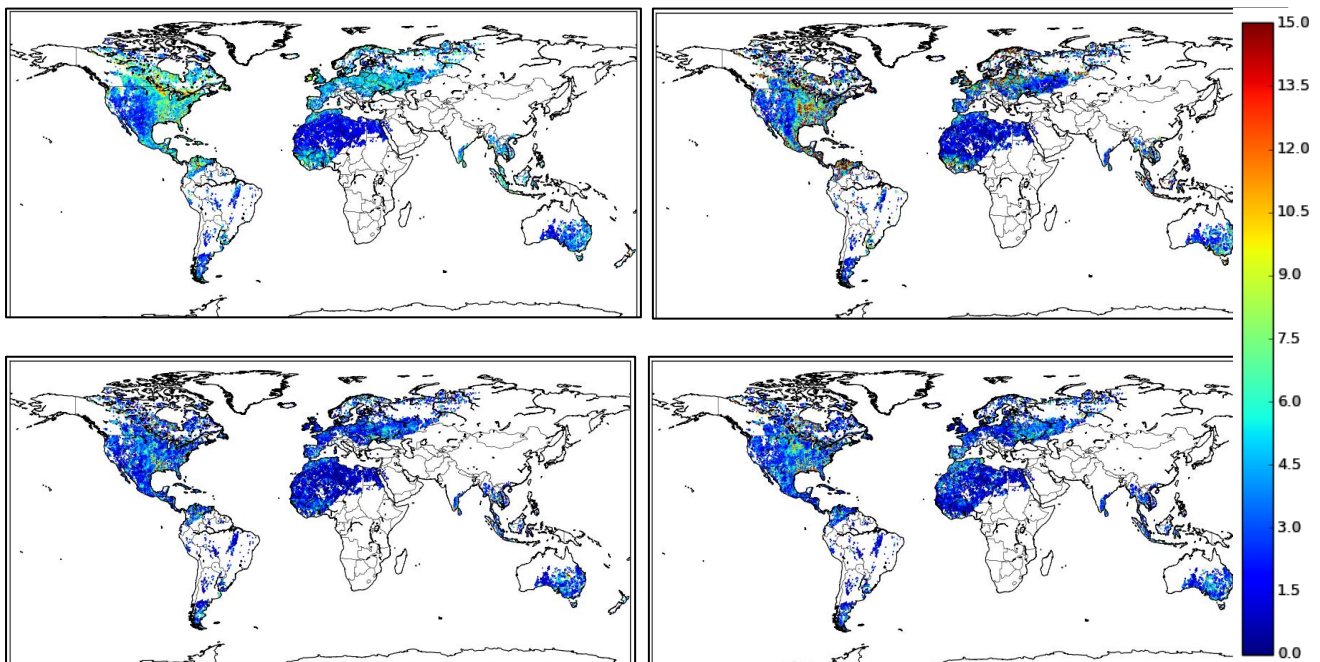


Fig.11: Error standard deviations in % of SMOS (on side left of first row), AMSR-E (on the right side of first row), ERA-Interim/Land (on the right side of the lower row) and ERS-2 (on the left side of the lower row) evaluated through the Extended Collocation technique considering a cross-correlation error between the radiometers.

In general, the error standard deviations maps estimated by the QC and the EC (considering a cross-correlation error between the two radiometers) showed similar patterns. Obviously, the absolute values of the error standard deviations changed and their means are reported in Table 4, considering the same macroareas of Table 2 and Table 3 for consistency. Focusing only on the SMOS, ERS-2 and model cases, the EC error standard deviation results shows similar trends respect to those obtained through the TC approach. Such outcome could be addressed to the probable presence of the error cross-correlation between the two radiometers, that should be considered.

Table 4: mean of the EC error standard deviations of SMOS, AMSR-E, ERA/Interim-Land and ERS-2 ESCAT soil moisture products depending on the considered area of the world.



World Area	SMOS [%]	AMSR-E [%]	ERA/Interim-Land [%]	ERS-2 [%]
Europe and Northern Africa	4.03	4.17	3.06	2.90
Northern America	4.10	4.49	3.41	3.16
Australia	2.92	3.03	2.61	3.31

The difference maps between the QC and EC error standard deviation estimations, reported in Fig.12, are very much related to the cross-correlation map reported in Fig.10. For instance, where the EC approach estimated an high cross-correlation error, the QC error standard deviation of SMOS was lower with respect to that provided by the EC.

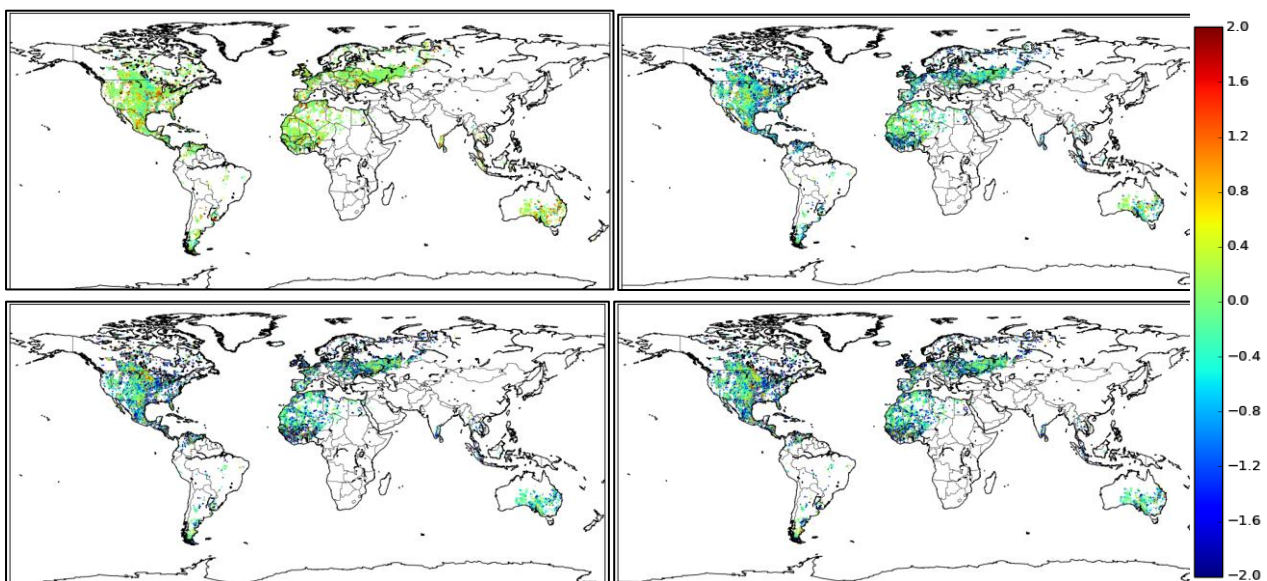


Fig.12: differences between the error standard deviations estimated through the QC and the EC approach for SMOS ( $\Delta\epsilon_{SMOS}$ , on the left side of the first row), AMSR-E ( $\Delta\epsilon_{AMSR-E}$ , on the right side of the first row), ERA/Interim-Land ( $\Delta\epsilon_{ERA}$ , on the left side of the second row) and ERS-2 ( $\Delta\epsilon_{ERS-2}$ , on the right side of second row).

As for the previous cases, the analysis was carried out considering both the ERS-2 data at nominal and high resolution. The histogram of the pointwise differences between

the estimated error standard deviations of each system is reported in Fig.13; the mean values for each distribution was -0.03, 0.03, 0.07 and 0.17 for SMOS, AMSR-E, ERA/Interim-Land and ERS-2 data, respectively.

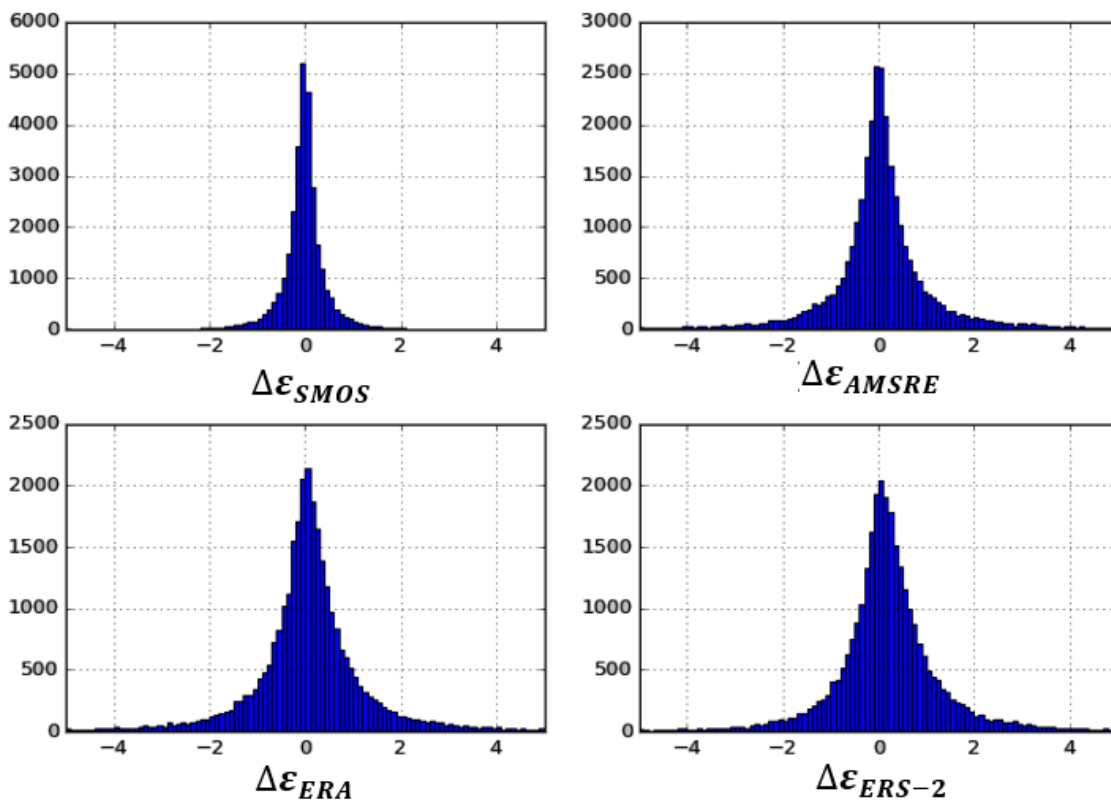


Fig.13: Histogram of the error standard deviation differences for SMOS ( $\Delta\epsilon_{SMOS}$ , on the left side of upper row), AMSR-E ( $\Delta\epsilon_{AMSR-E}$ , on the right side of upper row), ERA/Interim-Land ( $\Delta\epsilon_{ERA}$ , on left of lower row) and ERS-2 ( $\Delta\epsilon_{ERS-2}$ , on the right side of lower row) products; the differences were evaluated considering the EC results using ERS-2 at high resolution minus the EC results using the nominal ERS-2 products.

Once again, the distributions of the ERS-2 ESCAT differences between the error standard deviations (high resolution minus nominal resolution) confirmed the trend observed by the TC analysis.

### Global Average Analysis

Table 5 reports the worldwide mean of the error standard deviations evaluated for each system through the TC, QC and EC techniques, considering the ERS-2 ESCAT products at nominal resolution. Moreover, the EC approach was also applied to the systems supposing an error cross-correlation between SMOS and ERS-2 products.

Table 5: worldwide mean of the error standard deviations evaluated for SMOS, AMSR-E, ERA/Interim-Land and ERS-2 ESCAT soil moisture products through TC, QC and EC approaches. For the EC cases, the couple in the brackets indicates the position of the supposed error cross-correlation.

Method	SMOS [%]	AMSR-E [%]	ERA/Interim-Land [%]	ERS-2 [%]
TC	3.84	-	4.84	4.22
QC	3.45	4.79	5.54	4.62
EC <sub>[SMOS,AMSR-E]</sub>	3.84	4.44	3.36	2.91
EC <sub>[SMOS,ERS-2]</sub>	3.58	2.95	3.29	3.98

Analysing the line of the QC results, it can be noted as the error standard deviations of the model and the scatterometer worsen respect to those derived by the TC analysis. As previously mentioned in the text, such effect could be related to the possible presence of an error cross-correlation between the two radiometers. Indeed, if the EC was applied considering an error cross-correlation between SMOS and AMSR-E, the error standard deviations of the model and scatterometer improve respect to the previous estimates. A change in the trend of the results can be observed from the last line of Table 5, where an error cross-correlation between SMOS and ERS-2 ESCAT was considered; the results are influenced by the choice of the systems presenting an error cross-correlation. However, observing the trend of the error standard deviations and, in particular, the best performance of AMSR-E product respect to the other systems, the estimates considering an error cross-

correlation between the two radiometers seems to be more consistent than those obtained in the second analysed case of EC.

## **Conclusions**

In this work, soil moisture products produced by active and passive sensors were analysed at global scale. In particular, the ERS-2 ESCAT soil moisture retrievals, derived by the WARP processor (version 5.6), were compared with those produced by the ERA/Interim-Land model and by the two radiometers on-board the satellites SMOS (processor version 6.20) and AMSR-E (LPRM v5). For the ERS-2 ESCAT data, both the retrievals at high and nominal resolution were used for the comparison. The analysis covered a period of 18 months, starting from January 2010 to July 2011; such time limit was constrained by the satellite missions overlapping.

The Triple and Quadruple Collocation were applied to the datasets in order to estimate the error standard deviations of each system, and subsequently the Extended Collocation approach was applied to take in account the possibility of a cross-correlation error between the soil moisture estimates provided by the two radiometers. In general, the trend of the error standard deviations presented a coherent behaviour for all three analysis.

As a first step, the ERS-2 ESCAT soil moisture retrievals were compared with those produced by SMOS and ERA/Interim-Land model. From the pointwise correlation maps, it was possible to observe a dependence of the correlation behaviour with respect to soil cover, showing highest agreement over not densely vegetated area.

From the TC analysis, SMOS showed good performances over sparse vegetation cover, in particular over specific land cover (i.e., bare areas, shrubland and grassland). On the other side, the scatterometer and the model presented lowest error standard deviations over moderately vegetation covers. Such trend of the results were also confirmed by several literature works, which analysed soil moisture retrievals provided by active and passive satellite sensors. In general, the QC analysis

provided the same TC error patterns, showing low performance for AMSR-E in the North-East of United States, which is a region characterized by moderately to densely vegetated areas. Moreover, the error behaviours were also evaluated through the EC approach, considering cross-correlation error between the soil moisture estimations provided by the two radiometers. Once again, the trend of the results confirmed the patterns obtained by the TC analysis. Moreover, the similarity between the trends of the means of the TC and EC error standard deviations of SMOS, ERA/Interim-Land and ERS-2 data suggested that a cross-correlation error between the radiometers should be taken into account.

As already mentioned, all the approaches were carried out considering both the ERS-2 data at high and nominal resolution. From the analysis of the distribution of the pointwise differences between the error standard deviations of each system (depending on the resolution of the used scatterometer data), it was possible to note that the nominal ERS-2 retrievals provide a low standard deviation error with respect to those at high resolution. However, such trend is not representative of the best performances of the nominal ERS-2 products, but this result can be addressed to the resolution of the other systems. Indeed, the SMOS, AMSR-E and model resolution are more similar to that of the nominal ERS-2 data and the products at high resolution could be seen more noisily from the TC, QC and EC techniques with respect the other systems, if a spatial error is not considered into the error model.

## References

Al-Yaari, A., Wigneron, J.-P., Ducharne, A., Kerr, Y.-H., Wagner, W., De Lannoy, G., Reichle, R., Al Bitar, A., Dorigo, W., Rochaume, P., Mialon, A., "Global-scale comparison of passive (SMOS) and active (ASCAT) satellite based microwave soil moisture retrievals with soil moisture simulations (MERRA-Land)", *Remote Sensing of Environment*, 152, pp. 614-626, 2014.

Balsamo, G., Albergel, C., Beljaars, A., Boussetta, S., Brun, E., Cloke, H., ... Vitart, F., "ERA-Interim/Land: a global land-surface reanalysis based on ERA-Interim meteorological forcing", *Hydrology and Earth System Sciences*, 19, pp. 389–407, 2015, <http://dx.doi.org/10.5194/hess-19-389-2015>.

Dorigo, W.A., Scipal, K., Parinussa, R.M., Liu, Y.Y., de Jeu, R.A.M., and Naeimi, V., "Error characterisation of global active and passive microwave soil moisture datasets", *Hydrology and Earth System Sciences*, 14, pp. 2605-2616, 2010.

Gruber, A., Su, C.-H., Zwieback, S., Crow, W., Dorigo, W., Wagner, W., "Recent advances in (soil moisture) triple collocation analysis", *International Journal of Applied Earth Observation and Geoinformation*, 45, pp. 200-211, 2016.

Gruber, A., Su, C.-H., Crow, W.T., Zwieback, S., Dorigo, W.A., Wagner, W., "Estimating error cross-correlations in soil moisture data sets using extended collocation analysis", *Journal of Geophysical Research – Atmospheres*, 121(3), pp. 1208-1219, 2016.

Kerr, Y. H., Waldteufel, P., Richaume, P., Wigneron, J. P., Ferrazzoli, P., Mahmoodi, A., ..., Delwart, S., "The SMOS soil moisture retrieval algorithm", *IEEE Transactions on Geoscience and Remote Sensing*, 50, pp. 1384–1403, 2012, <http://dx.doi.org/10.1109/TGRS.2012.2184548>.

Kerr, Y., Waldteufel, P., Wigneron, J. -P., Martinuzzi, J. -M., Font, J., & Berger, M., "Soil moisture retrieval from space: the Soil Moisture and Ocean Salinity (SMOS) mission", *IEEE Trans. Geosci. Remote Sensing*, 39, pp. 1729–1736, 2001.

Kidd, R. A., "Implementation plan for a NRT global ASCAT soil moisture product for NWP, part 4: discrete global grid systems", *NWP SAF (Satellite Application Facility for Numerical Weather Prediction Associate Scientist Mission Report)*, 2005.

Miralles, D.G., Crow, W.T., Cosh, M.H. "Estimating Spatial Sampling Errors in Coarse-Scale Soil Moisture Estimates Derived from Point-Scale Observations", *Journal of Hydrometeorology*, 11, pp. 1423-1429, 2010.



Owe, M., de Jeu, R., and Walker, J., “A methodology for surface soil moisture and vegetation optical depth retrieval using the Microwave Polarisation Difference Index”, *Geosci. Remote Sens.*, 39 (8), pp. 1643-1654, 2001.

Pierdicca, N., Fascetti, F., Pulvirenti, L., Crapolicchio, R., Munoz-Sabater, J., “Analysis of ASCAT, SMOS, in-situ and land model soil moisture as a regionalized variable over Europe and North Africa”, *Remote Sensing of Environment*, 170, pp.280-289, 2015.

Pierdicca N., Fascetti, F., Pulvirenti, L., Crapolicchio, R., Mnuoz-Sabater, J., “Quadruple Collocation Analysis for Soil Moisture Product Assessment”, *IEEE Geoscience and Remote Sensing Letters*, 12, p., 1595-1599, 2015.

Wagner, W., Lemoine, G., & Rott, H., “A method for estimating soil moisture from ERS scatterometer and soil data—empirical data and model results”, *Remote Sensing of Environment*, 70, pp. 191–207, 1999.